Detection of Partially Fallen-Out Magnetic Slot Wedges in Inverter-Fed AC Machines at Lower Load Conditions

Goran Stojčić, Mario Vašak, *Member, IEEE*, Nedjeljko Perić, *Senior Member, IEEE*, Gojko Joksimović, *Senior Member, IEEE*, and Thomas M. Wolbank, *Member, IEEE*

***Abstract*—Electrical machines in the high-voltage class are usually designed with open stator slots. This wide open slots cause an increase of higher order harmonics, vibrations, noise, and temperature; thus, the machine efficiency is decreased. To counteract this disadvantage, magnetic slot wedges are applied. Due to the impact of high magnetic and mechanical forces, these wedges can fall out and may cause further serious damages. Up to now, reliable detection methods for single missing slot wedges are coupled with a disassembling of parts of the machine. In this paper, a method is investigated which provides the possibility of detection, based on the measurement of electrical terminal quantities only.**

***Index Terms*—AC machines, condition monitoring, fault detection, stator slot wedges, transient excitation.**

I. Introduction

In HIGH-POWER and high-voltage machines, the stator slots are usually wide open. This design scheme is a consequence of the assembling process of the fully formed winding coils. The open-slot structure does, however, carry a number of disadvantages compared to the semiclosed slots of machines with lower power and voltage rating. The main disadvantages are higher harmonic components in the air gap field, uneven flux distribution, vibration between the stator and rotor, increased magnetizing current, and higher noise levels. As a consequence, losses are increased, and the power factor and efficiency are decreased [1], [2]. To reduce these drawbacks, magnetic stator slot wedges are applied to the stator slots. Therewith, the flux density is becoming smoother, and the magnetizing current is lower due to the reduced effective air gap field [3]. Another benefit is the reduction of the inrush and starting current and increase of the starting torque [4], [5].

Industrially applied magnetic wedges are usually composed of iron powder glass mat and resin. As a result, conductivity is thus very low, and thus, also the core losses can be significantly decreased [2], [6], [7].

The machine's lamination, stator windings, and magnetic wedges are exposed to high magnetic and mechanical forces. These forces may lead to vibrations between wedges and stator notches and cause a loosening of the wedges. In particular, a high number of motor starts, operation above the rated load, and pulsating load profiles affect an increase of these forces. The so-caused loosened wedges may fall out into the air gap and are either directly grinded down to powder or eventually lead to further damages. To achieve the high reliability and high efficiency of the machine, all machine components have thus to be monitored. Due to the properties of the slot wedges, a monitoring system for these components is extremely challenging. Nowadays, available standard detection methods suffer from the drawback that the identification of loosen or missing slot wedges is coupled with the partial disassembling of the machine [8]. This can cause higher financial burden as well as higher downtimes of drives and systems. Hence, methods must be developed able to detect missing slot wedges without machine disassembling. In [8], it was reported that there are hardly known methods dealing with this issue. Basically, all methods known for the detection of machine asymmetries can be taken into consideration (e.g., current signature analysis, Park's vector approach, etc.). However, due to the known issues with spectrum analysis in combination with inverter-fed operation as well as the relative low influence of missing magnetic wedges on the fundamental-wave characteristic of electric machines, new developed methods should preferably be focused on the high-frequency or transient electrical machine properties.

In this paper, a method for the detection of missing stator slot wedges without the need of machine dissembling is investigated [9]. The method is based on the examination of the machine's transient reactance. By applying short voltage pulses to the machine terminals using an inverter, a transient excitation is achieved. The measurement of the current response and a subsequent signal processing of the obtained values provide a fault indicator to detect missing slot wedges based only on machine electrical quantities. The main focus of this paper is placed on the verification of the detection sensitivity as well as on the method's applicability while the machine is in operation.

Manuscript received November 14, 2012; revised April 23, 2013 and June 4, 2013; accepted June 9, 2013. Date of publication August 1, 2013; date of current version March 17, 2014. Paper 2012-IPCC-631.R2, presented at the 2012 IEEE Energy Conversion Congress and Exposition, Raleigh, NC, USA, September 15–20, and approved for publication in the IEEE Transactions on Industry Applications by the Industrial Power Converter Committee of the IEEE Industry Applications Society. This work was supported by the European Union within the SEE-ERA.NET PLUS framework.

G. Stojčić is with the Department of Energy Systems and Electrical Drives, Vienna University of Technology, 1040 Vienna, Austria (e-mail: goran.stojcic@tuwien.ac.at).

M. Vašak and N. Perić are with the Faculty of Electrical Engineering and Computing, University of Zagreb, HR-10002 Zagreb, Croatia (e-mail: mario.vasak@fer.hr; Nedjeljko.peric@fer.hr).

G. Joksimović is with the Faculty of Electrical Engineering, University of Montenegro, 81000 Podgorica, Montenegro (e-mail: joxo@ac.me).

T. M. Wolbank is with the Faculty of Electrical Engineering and Information Technology, Vienna University of Technology, 1040 Vienna, Austria (e-mail: thomas.wolbank@tuwien.ac.at).

Color versions of one or more of the figures in this paper are available online at http://ieeexplore.ieee.org.

Digital Object Identifier 10.1109/TIA.2013.2275955

II. Machine Transient Reactance

When applying transient pulse voltage signals to the terminals, the response will be a current slope which is dominated by the machine parameters. In the first transient reaction, the dominating parameter is the transient leakage inductance. An essential part of the leakage flux is the stator slot leakage and the zigzag leakage flux. The leakage flux paths are basically predefined by the slot wedges. Assuming one or more missing wedges, a significant change of the leakage flux path is given with respect to the faultless symmetrical case, and thus, the transient leakage inductance will change. This variation can be detected by the obtained current slope and additional signal processing steps. However, not only missing slot wedges but also other types of faults (e.g., air gap eccentricity and interturn short circuit) can cause a transient leakage inductance modification and are thus detectable with the proposed method.

A simple and effective way to establish the transient excitation is realized by applying short voltage pulses generated by a standard industrial inverter. Changing from inactive to any active inverter state provides a voltage step with the magnitude of the dc-link voltage. Due to the fact that only a short time trace of the current response is needed, the voltage excitation can be realized as very short pulses of some 10-μs duration only. Therefore, the inverter is switched from inactive to active and back again. The current slope measurement can then be easily realized within the pulse duration by the inverter built-in current sensors. Thus, no special measurement hardware is needed, and costs can be kept low. Furthermore, the measurements are done offline at zero flux and no load; hence, the power rating of the inverter can be reduced to a fraction of the machine's rated power.

The machines electrical behavior is described with the well-known stator equation in space phasor representation

$$\underline{v}_S = r_S \cdot \underline{i}_S + l_l \cdot \frac{d\underline{i}_S}{d\tau} + \frac{d\underline{\lambda}_R}{d\tau}. \tag{1}$$

The three voltage drops which influence the current reaction within the voltage excitation $\underline{v}_S$ are determined by the parameters stator resistance r_S, leakage inductance l_l, and back electromotive force (EMF) $(d\lambda_{\mathrm{R}}/d\tau)$. The identification of the leakage inductance is challenging due to the disturbances of the back EMF and stator resistance. An accurate identification of the leakage inductance is thus only possible after the elimination of both disturbing voltage drops.

Considering now a short voltage pulse v applied by inverter switching in one phase direction, the machine's response will be a current slope (di/dt), as shown in Fig. 1. Due to the discrete nature of the measurement, the current slope is approximated by (2), and the mean current value i_{mean} is calculated by (3)

$$\frac{di}{dt} \approx \frac{i_2 - i_1}{\Delta\tau} = \frac{\Delta i}{\Delta\tau} \tag{2}$$

$$i_{\mathrm{mean}} = \frac{i_1 + i_2}{2}. \tag{3}$$

Applying now a subsequent second voltage pulse in the opposite direction, the current slope will have the same slope, but opposite in sign. The value of i_{mean} will thus be almost

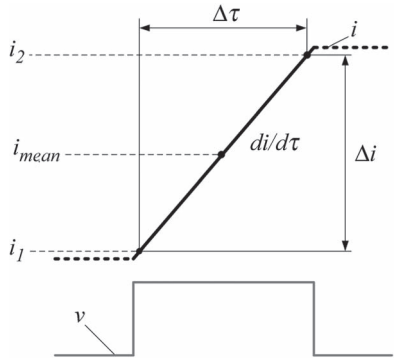

Fig. 1. Phase current response to an applied voltage step in one phase direction.

equal for both pulses. Considering now these coherences in the space frame representation, the voltage pulses can be denoted as $\underline{v}_{S,I}, \underline{v}_{S,II}$, and the current slope can be denoted as $\Delta\underline{i}_I$, $\Delta\underline{i}_{II}$, respectively. As the voltage pulse duration is only some 10 μs and the pulses are applied immediately after each other, the fundamental-wave operating point will not change significantly, and $\underline{i}_S$ can be approximated by i_{mean}. Furthermore, the magnitude and direction of back EMF can be considered as constant $(d\underline{\lambda}_{\mathrm{R,I}}/d\tau \sim d\underline{\lambda}_{\mathrm{R,II}}/d\tau)$ as for the dc-link voltage. The subtraction of the voltage pulses (1) leads to (4) with the assumptions mentioned earlier. The voltage drops effected by stator resistance and back EMF are thus eliminated as indicated in (4), and parameter variations like stator resistance temperature dependence can be neglected

$$\underline{v}_{S,I} - \underline{v}_{S,II} = \overbrace{r_S \cdot \underline{i}_{S,I} - r_S \cdot \underline{i}_{S,II}}^{\approx 0} + l_{l,t} \cdot \frac{\Delta\underline{i}_{S,I}}{\Delta\tau} - l_{l,t} \cdot \frac{\Delta\underline{i}_{S,II}}{\Delta\tau} + \underbrace{\frac{d\underline{\lambda}_{R,I}}{d\tau} - \frac{d\underline{\lambda}_{R,II}}{d\tau}}_{\approx 0}$$

$$\underline{v}_{S,I} - \underline{v}_{S,II} = l_{l,t} \cdot \left[\frac{\Delta\underline{i}_{S,I}}{\Delta\tau} - \frac{\Delta\underline{i}_{S,II}}{\Delta\tau}\right]. \tag{4}$$

Up to now, a symmetrical machine has been assumed with the leakage inductance equal to the transient inductance. Due to the fact that the transient inductance differs from the fundamental-wave leakage inductance, the notation will be changed to $\underline{l}_{\mathrm{l,t}}$ in the following. Furthermore, the inductance was assumed to be a scalar value. This assumption only holds if the current slope and the excitation voltages have the same direction. Considering now a real machine, faulty or not, the two directions will no longer be exactly the same. Thus, in (4), the transient inductance $l_{\mathrm{l,t}}$ will no longer be a scalar value but a spatial complex one. This results from the phase values of the transient inductance being no longer equal. As a result, the directions of the voltage difference phasor $\underline{v}_{\mathrm{S,I-II}}$ and current derivative difference phasor $\Delta\underline{i}_{\mathrm{S,I-II}}/\Delta\tau$ will no longer be the same. The so-introduced complex transient inductance $\underline{l}_{\mathrm{l,t}}$ is composed of a scalar portion l_{offset} and a complex portion $\underline{l}_{\mathrm{mod}}$ (5). The "offset" part is representing the symmetrical portion of the asymmetrical machine, and the "mod" part is representing the modulation due to asymmetry. The magnitude

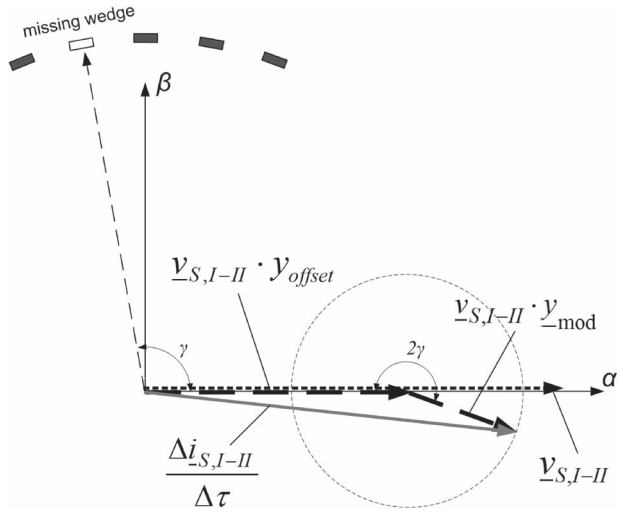

Fig. 2. Pulse excitation and resulting current change in the presence of a missing slot wedge.

and angle of $\underline{l}_{\mathrm{mod}}$ contain the information about the asymmetry. The angle γ represents the spatial position of the inductance's maximum within one pole pair. In case of a missing stator slot wedge, the maximum inductance will point in this direction. The magnitude of $\underline{l}_{\mathrm{mod}}$ will also increase in that case. Therefore, the observation of $\underline{l}_{\mathrm{mod}}$ provides information about missing stator slot wedges

$$\begin{aligned} \underline{l}_{l,t} &= l_{\mathrm{offset}} + \underline{l}_{\mathrm{mod}} \\ \underline{l}_{\mathrm{mod}} &= l_{\mathrm{mod}} \cdot e^{j2\gamma}. \end{aligned} \tag{5}$$

As shown in (4), it is sufficient to monitor the resulting current slope to calculate the angular position of the maximum inductance. This can be achieved if (5) is inserted in (4) with $\underline{l}_{\mathrm{l,t}}$ replacing $l_{\mathrm{l,t}}$ and subsequent inversion, which leads to (6) with $\underline{y}_{\mathrm{l,t}} = 1/\underline{l}_{\mathrm{l,t}}$. Therewith, the number of mathematical calculations is reduced, and the measurement/control system need not carry out divisions

$$\frac{\Delta \underline{i}_{S,I-II}}{\Delta \tau} = \underline{y}_{l,t} \cdot \underline{v}_{S,I-II} = \left[y_{\mathrm{offset}} + \underline{y}_{\mathrm{mod}} \right] \cdot \underline{v}_{S,I-II}. \tag{6}$$

In Fig. 1, the coherences of all parameters are shown for an excitation with a voltage difference phasor $\underline{v}_{\mathrm{S,I-II}}$ in phase direction U (dotted black phasor) in the stator fixed frame (α, β). This excitation is obtained by two subsequent pulses, one pointing in the positive direction of phase U and the other pointing in the negative direction. The position of the missing slot wedge was assumed with an angle of $\gamma = 100°$ with respect to the phase direction U. As shown in Fig. 2, the resulting current change phasor $\Delta i_{\mathrm{S,I-II}}/\Delta\tau$ (gray phasor) is composed of an "offset" part and a "mod" part. Both portions are shown as black dashed phasors and denoted with $\underline{v}_{\mathrm{S,I-II}} \cdot y_{\mathrm{offset}}$ and $\underline{v}_{S,I-II} \cdot \underline{y}_{mod}$, respectively. The offset portion points in the excitation direction, and the modulated portion has an angular direction of twice the angle γ. For the transient leakage inductance, it is not essential if the missing slot wedge is located in the positive or negative phase direction. Thus, $\underline{l}_{\mathrm{mod}}$ has a maximum in the direction of the missing wedges as well as in the opposite direction, and the period is twice that of the fundamental wave. The obtained current slope after the measurement and signal processing is thus the summation of the symmetrical and the fault-induced portion.

If the direction of the asymmetry is the same as the direction of the resulting excitation voltage $\underline{v}_{S,I-II}(\gamma = 0°, \gamma = 180°)$, the resulting current slope obtained has the same direction as the applied resulting voltage as if the machine was symmetrical. However, compared to the symmetrical portion, its magnitude is smaller. With an angular asymmetry difference of $\gamma = 90°$, again, the same "symmetrical" direction is obtained but with higher magnitude. Obviously, the tip of the fault-induced phasor $(\underline{v}_{\mathrm{S,I-II}} \cdot \underline{y}_{\mathrm{mod}})$ moves along the dotted circle twice when the position of the missing slot wedge is changed over one electrical period. However, before the obtained current slope can be used to detect missing slot wedges, some further specific signal processing steps have to be executed to achieve a fault indicator with necessary high accuracy.

III. Signal Processing for Fault Indicator Calculation

A. Elimination of the Symmetrical Portion

In the previous section, it was shown that the modulated part of the complex transient leakage inductance corresponds with missing slot wedges. The current slope resulting from voltage pulse excitation is thus a well-suited measurement signal for the determination of such faults. Before exploiting this information to develop a fault indicator, some disturbing signal components have to be eliminated. In every machine, faultless or not, the symmetrical part in the current response signal is predominant. Usually, this part is responsible for about 90% of the overall resulting current change phasor, as presented in Fig. 3. Thus, it is clear that the symmetrical portion has to be eliminated to obtain a high sensitive fault indicator. The elimination can be done using a voltage excitation sequence that sequentially changes its resulting direction $(\underline{v}_{\mathrm{S,I-II,U}}, \underline{v}_{\mathrm{S,I-II,V}}, \underline{v}_{\mathrm{S,I-II,W}})$ in the main three phase axes. Thus, three different current change phasors are obtained $(\Delta \underline{i}_{\mathrm{S,I-II,U}}/\Delta\tau, \Delta \underline{i}_{\mathrm{S,I-II,V}}/\Delta\tau, \Delta \underline{i}_{\mathrm{S,I-II,W}}/\Delta\tau)$, each with the symmetrical portion pointing in one main phase direction (see Fig. 3). Combining the current change phasors of each phase to one resulting phasor, the share of the symmetrical machine (7) leads to a zero sequence and is eliminated (8). The remaining phasor $\underline{C}$ after carrying out this step now only contains information on machine asymmetries and will be denoted as the asymmetry phasor in the following:

$$y_{\mathrm{offset},U} \approx y_{\mathrm{offset},V} \approx y_{\mathrm{offset},W} \tag{7}$$

$$\begin{aligned} \underline{C} &= \frac{\Delta \underline{i}_{S,I-II,U}}{\Delta \tau} + \frac{\Delta \underline{i}_{S,I-II,V}}{\Delta \tau} + \frac{\Delta \underline{i}_{S,I-II,W}}{\Delta \tau} = \ldots \\ &= \underline{y}_{\mathrm{mod},U} \cdot \underline{v}_{S,I-II,U} + \underline{y}_{\mathrm{mod},V} \cdot \underline{v}_{S,I-II,V} \\ &\quad + \underline{y}_{\mathrm{mod},W} \cdot \underline{v}_{S,I-II,W}. \end{aligned} \tag{8}$$

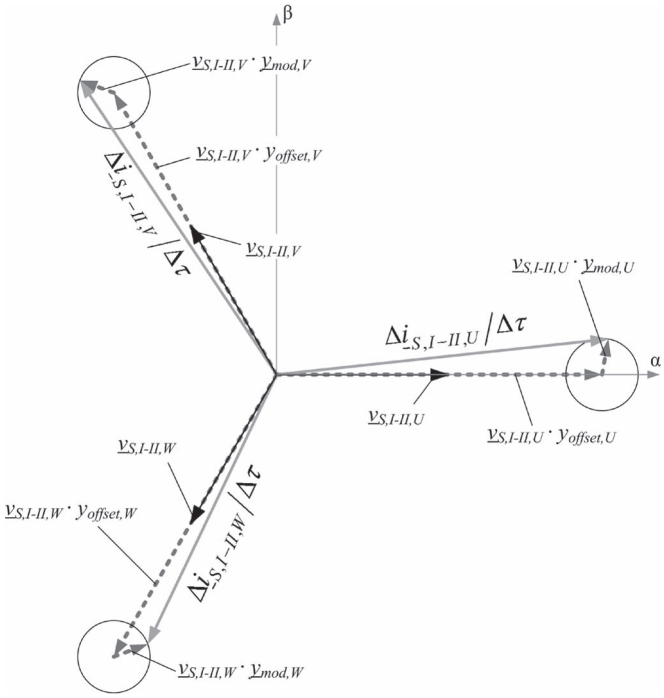

Fig. 3. Relations of the symmetrical (90%) and the modulated (10%) portion corresponding to the voltage pulses in the main phases. The voltage phasors are clearly reduced to improve visibility.

B. Fault Indicator Calculation

The asymmetry phasor serves as the base for the fault indicator. However, the asymmetry phasor not only consists of fault-induced modulations but also contains some inherent asymmetries. These inherent parts superpose and thus clearly reduce the indicator's accuracy. However, separation is still possible due to the deterministic behavior of each inherent asymmetry. The main inherent asymmetries are caused by spatial saturation and rotor slotting. Saturation saliency arises from different levels of saturation of the lamination material along the circumference caused by the fundamental wave. The period of this asymmetry corresponds to the number of poles and is twice that of the fundamental wave. Another inherent asymmetry is the slotting saliency which is caused by the openings of the slots in the lamination. Its period is linked to the mechanical rotor angle and equals the number of rotor slots. Basically, this description of inherent saliencies is limited to a squirrel cage induction machine because this investigation focuses on that machine type. Nevertheless, it can be adapted also to other types of ac machines like permanent-magnet synchronous machines.

For the separation of the mentioned asymmetries, some specific signal processing steps have to be carried out. To get a clearer presentation of the separation process Fig. 4 shows the data acquisition and fault indicator estimation as a block diagram. Different steps are executed as described in the following. The measurement control unit decides when a measurement process starts and triggers the asymmetry phasor estimation. In the figure, this part is marked with the dashed box. The machine is excited by voltage pulses applied, and the current response within the pulse duration is measurement. Subsequently, the asymmetry phasor is calculation as described earlier. The voltage pulses are applied subsequent to the main three phase

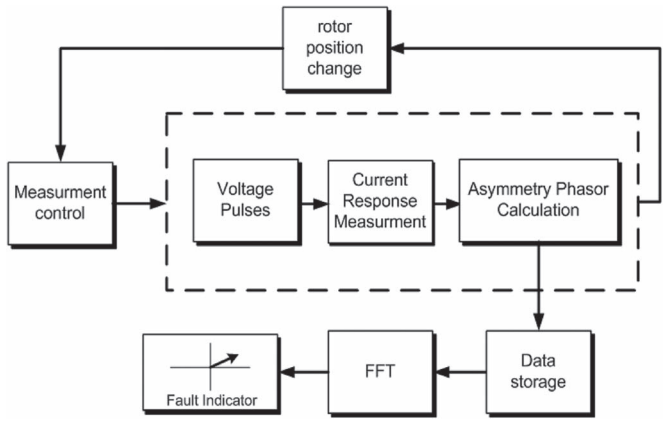

Fig. 4. Block diagram of data acquisition and fault indicator calculation process.

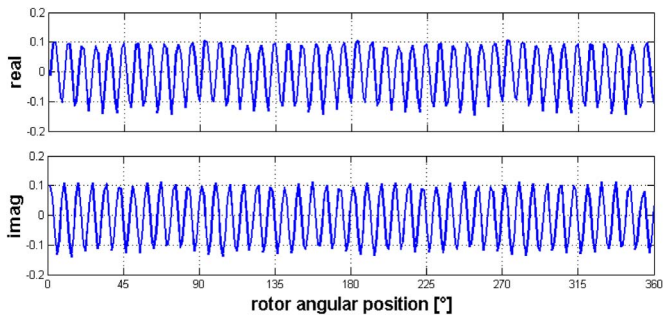

Fig. 5. Asymmetry phasor signal for one rotor revolution.

directions, so three current change phasors ($\Delta \underline{i}_{S,I-II}/\Delta\tau$) are obtained. By adding them into one resulting phasor, the symmetrical portion $\underline{v}_{\mathrm{S,I-II}} \cdot y_{\mathrm{offset}}$ is eliminated. Subsequently, the obtained asymmetry phasor is forwarded to the data storage block. This storage is realized as a vector array whose elements correspond to specific rotor positions. The respective rotor positions can be obtained from the control algorithm or by a manual evaluation. The asymmetry phasor is stored in the corresponding element. Meanwhile, the rotor position is changed. This can be done manually, by load, or using the inverter. After that, the procedure is repeated, and a new asymmetry phasor is obtained and stored. The whole process is repeated for at least one rotor slotting period. To achieve a higher resolution, a set of asymmetry phasors is collected for one mechanical revolution of the rotor. Thus, a multiple of periods of all rotor fixed saliencies is obtained. Fig. 5 presents the asymmetry phasor signal for one mechanical rotor revolution.

The set of asymmetry phasors is then forwarded from the data storage to the FFT block where the separation of all asymmetries is realized. Due to the window length being a multiple of the rotor fixed saliency periods, a clear identification and elimination of these modulations is realized. If the spectral filtering is used to eliminate also the saturation saliency (when present in a magnetized induction machine or a permanent-magnet machine), then the FFT has to be repeated with the window length chosen to a multiple of the saturation saliency period.

Considering the origin of the saliency induced from a missing slot wedge, it is obvious that the geometrical position of the asymmetry with respect to the stator does not change, and neither with the rotor angle nor with the fundamental-wave flux

TABLE I
PARAMETERS OF TEST MACHINE

Parameter	value
nominal voltage	450 V
nominal frequency	75 Hz
nominal current	19 A
number of pole pair	2
number of stator slots	36
stator resistance (phase)	0.147 Ω
stator inductance	72.5 mH
stator connection	Y

angle. As the pulse excitation and current measurement is stator fixed too, the offset component of the FFT thus corresponds to the slot wedge asymmetry and serves as a fault indicator. Due to the complex nature of the FFT, the fault indicator (offset component) has a magnitude and a direction. Both parameters are used to characterize a fault. Basically, this complex value is denoted as the fault indicator in the following.

IV. MEASUREMENT SETUP AND RESULTS

The measurement setup to verify the detection method consists of an 11-kW squirrel cage induction machine (parameters given in Table I), a voltage source inverter, and a measurement and control unit programmable under Matlab/Simulink. The current samples are measured by standard industrial current sensors. The test machine is a four-pole type with unskewed rotor bars, and the stator has 36 stator slots and full pitched windings. The wedges are made from standard industrial magnetic slot wedge material. The stator slot wedges are made of composite iron powder (75%), epoxy resin (18%), and glass mat (7%). Hence, the slot wedge permeability is high while the conductivity is kept low. Due to the fact that the stator of the test machine has semiclosed slots, the slot wedges are specially adapted to fit in these slots. Fig. 6 presents two close views of the stator, one with all wedges placed and another with one removed wedge. However, not only whole missing wedges can be realized; also, partially falling out wedges can be simulated by applying only parts of a wedge in the slots. Field experiences have shown that, usually, at first, not the whole but only one part of a wedge is missing [8]. This is caused by the fault development of missing slot wedges. In a first step, the slot wedge is getting loose on one end or in the center of the stator length. Due to the loosening of the wedge and impact of high magnetic and mechanical forces, the wedge starts vibrating and is pulled toward the air gap. Gradually, the vibration magnitude is getting higher. As a consequence, the wedge breaks, and one part falls out into the air gap while the other is still remaining in the slot.

A. Sensitivity Analysis

To test the sensitivity of the proposed method, a first set of measurements was done on a nonmagnetized machine with zero flux and no load. The measurement results are shown in Fig. 7. Results presented in the following show the method's accuracy as an offline procedure. The method is not only applicable for inverter-fed machines. It can also be adapted to mains-fed machines during maintenance work. Due to the complex nature

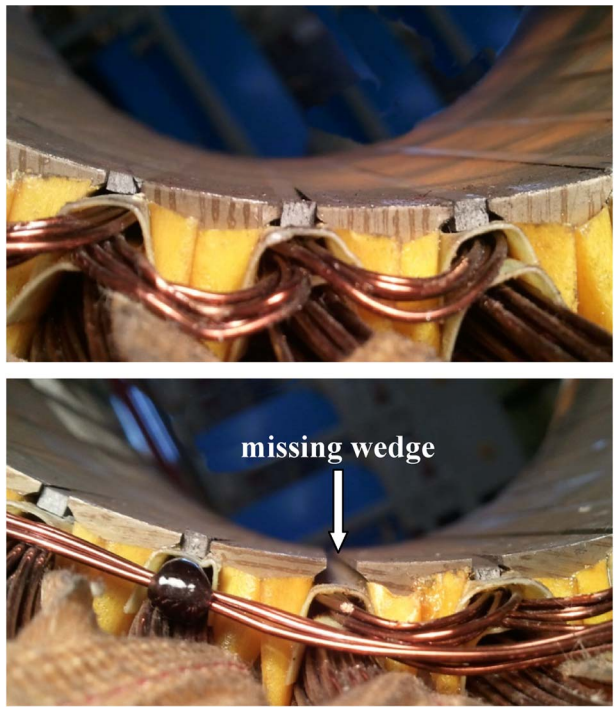

Fig. 6. Placed and the removed slot wedge in the test machine for simulation of missing wedge faults.

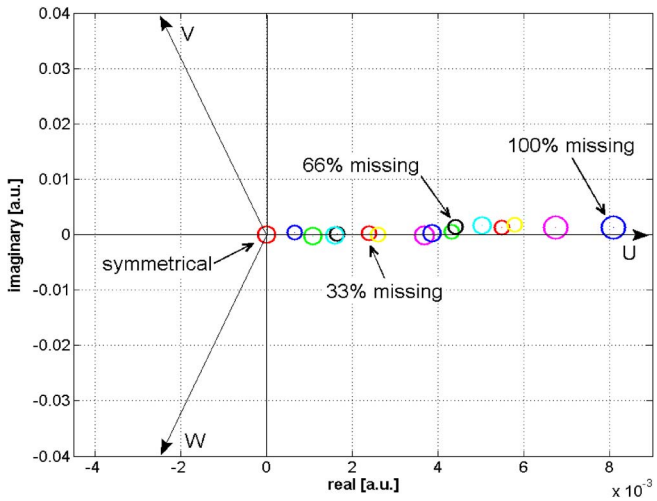

Fig. 7. Measurement results of sensitivity analysis for partially missing slot wedge in phase U.

of the asymmetry phasor and fault indicator, respectively, the results are given in the complex frame format. This is also a well-suited illustration to get a clear impression on fault magnitude and direction at once.

At the first set of measurements, the machine was tested for the symmetrical case. Thereby, all slot wedges were placed in the slot openings, and the fault indicator value here serves as the reference (denoted by "symmetrical") but differs already from the origin. This can be explained by stator fixed asymmetries like lamination anisotropy, current sensors, and distribution of the windings which cause an offset value. However, this value can be obtained in advanced and used for later elimination. A deviation of the fault indicator from the "new" origin now indicates a faulty slot wedge.

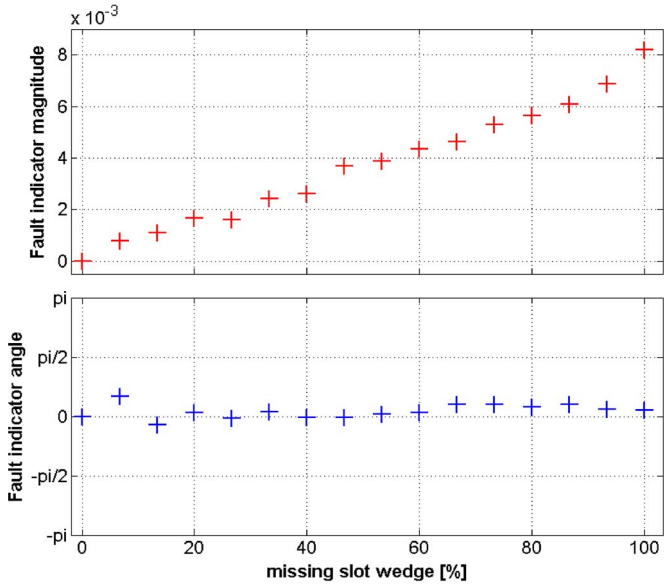

Fig. 8. Measurement results and accuracy of fault indicator versus the percentage of one missing slot wedge in phase direction U.

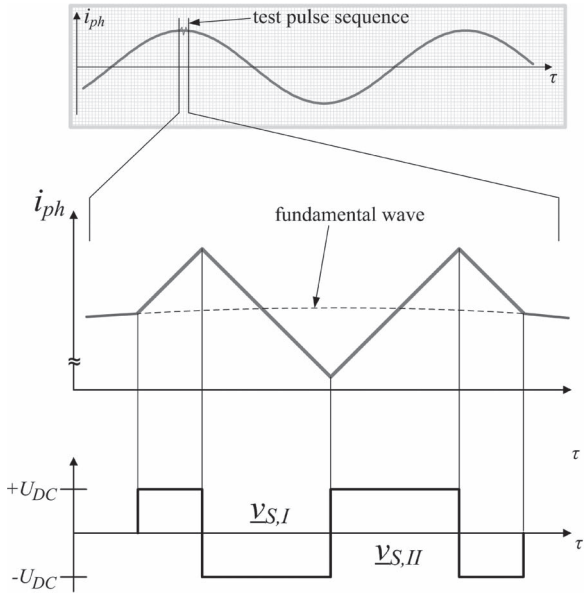

Fig. 9. Voltage pulse excitation signal during online detection.

In the following steps, only fractional parts of one wedge were removed from the stator lamination. The steps were portioned into 1/15 of the stator length. In each step, the fault indicator estimation was repeated 250 times to prove the fault indicator statistical distribution. All measurement results are shown as circles for each step. The circle's midpoint represents the mean value of all fault indicators, and the radius represents the maximum deviation. The axis values of the diagrams are given in arbitrary units corresponding to the internal representation of the digital signal processor. In Fig. 8, the fault indicator's magnitude and angle are plotted against the percentage of one missing stator slot wedge. The results presented in Fig. 7 show a clear coherence of the fault indicator magnitude and fault severity. Aside from the fault magnitude, also the fault position can be identified due to the movement of the fault indicator into the corresponding phase direction. It has, however, to be stressed that the direction in Figs. 7 and 8 only gives the spatial position within one pole pair. The ambiguity increases with the number of pole pairs.

B. Online Measurements

The investigation results and description in the following are limited to online inverter-fed operation. The machine is fed by a full-size inverter and operated by a field-oriented control scheme. The inverter control scheme is a standard pulsewidth modulation (PWM). The test machine was coupled to a load machine.

Due to the relative short time duration of the excitation voltage pulses (some 10 μs), the estimation procedure can be realized within one PWM cycle. During this estimation process, the current control is interrupted, and a special voltage pattern is applied which is shown in Fig. 9. The figure shows a cutout of one phase current signal. Aside from the applied test pulse sequence voltage signal, also the current reaction is presented schematically. The test pulse signal is a symmetrical time trace of the voltage $\underline{v}_{\mathrm{S}}$ in one phase direction. It consist of positive and negative switching states $(+,-,+,-)$. The resulting mean voltage during this period is thus zero.

Furthermore, also the current trace (gray line) is shown. The fundamental-wave point of operation is indicated by the dashed line. Due to the symmetrical nature of the excitation signal, the fundamental-wave point before and after the excitation period is almost unchanged due to that the current value returns to the fundamental-wave value. The applied voltage signal is a line-to-line voltage according to the inverter output voltage, the magnitude is equal to the dc-link voltage, and the whole duration was set to 200 μs, whereas the ratio between the short and long sequences is set to 0.5. It must be mentioned that this configuration is well suited for the presented test machine. When applying the method to other machines, the pulse duration has to be adapted. For high-speed machines with lower inductance, the pulse duration must be clearly reduced to avoid overcurrent during measurement.

Basically, the investigated fault cases in the section online measurements are done with fully removed slot wedges in phase direction U. Starting with only one removed wedge, the fault severity was increased by removing a second and, finally, a third slot wedge. To identify the fault indicator load dependence, the detection procedure was repeated at different load levels. Beginning with zero load, the load level was increased up to 60% rated load limited by the test machine configurations. Basically, the test machine is designed with semiclosed stator slots. The slot wedges were applied with a rectangular cross section and are fixed by a bonding material. Higher load levels introduce higher magnetic forces and, thus, the risk of slot wedge pullout. All fault indicator results are given in Fig. 10. The figure is given as a 3-D presentation of the fault indicator magnitude for different fault cases. The x-axis represents the load level in percent of the rated load. The y-axis corresponds to the number of missing slot wedges. Missing wedges are consecutive within the pole area of one phase. It can be seen that the fault indicator is almost independent of the machine load. A detection of missing slot wedges is thus also possible online during normal operation of the drive.

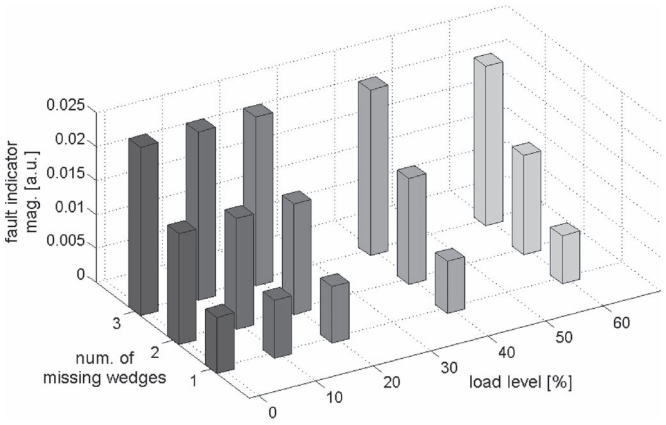

Fig. 10. Fault indicator dependence on machine load and number of missing wedges. The symmetrical case is represented by the x–y area.

V. Conclusion

A method has been investigated to detect missing and partially missing magnetic slot wedges in ac machines. The method provides the advantage that detection is possible without disassembling the machine. It can be applied offline at standstill as well as online during operation of the drive. The detection is based on the spatial properties of the transient leakage flux. These properties can be identified by a transient excitation of the machine with short voltage pulses. Measuring and subsequent signal processing of the resulting current response delivers a fault indicator with high accuracy of both fault severity and direction. The accuracy was proven for partially as well as whole missing slot wedges. Furthermore, applicability was verified offline on a nonmagnetized machine as well as online on a machine operated by an inverter with different load levels. The results have shown a high accuracy of the fault indicator even if only 1/15 of one wedge is missing.

References

[1] H. Mikami, K. Ide, K. Arai, M. Takahashi, and K. Kajiwara, "Dynamic harmonic field analysis of a cage type induction motor when magnetic slot wedges are applied," *IEEE Trans. Energy Convers.*, vol. 12, no. 4, pp. 337–343, Dec. 1997.

[2] R. Curiac and H. Li, "Improvements in energy efficiency of induction motors by the use of magnetic wedges," in *Proc. 58th Annu. IEEE PCIC*, Sep. 19–21, 2011, pp. 1–6.

[3] S. Wang, Z. Zhao, L. Yuan, and B. Wang, "Investigation and analysis of the influence of magnetic wedges on high voltage motors performance," in *Proc. IEEE VPPC*, Sep. 3–5, 2008, pp. 1–6.

[4] J. Kappatou, C. Gyftakis, and A. Safacas, "A study of the effects of the stator slots wedges material on the behavior of an induction machine," in *Proc. 18th ICEM 2008*, Sep. 6–9, 2008, pp. 1–6.

[5] K. N. Gyftakis, P. A. Panagiotou, and J. Kappatou, "The influence of semi-magnetic wedges on the electromagnetic variables and the harmonic content in induction motors," in *Proc. 20th ICEM*, Sep. 2–5, 2012, pp. 1469–1474.

[6] Y. Takeda, T. Yagisawa, A. Suyama, and M. Yamamoto, "Application of magnetic wedges to large motors," *IEEE Trans. Magn.*, vol. 20, no. 5, pp. 1780–1782, Sep. 1984.

[7] M. Davis, "Problem and solutions with magnetic stator wedges," in *Proc. Iris Rotating Mach. Conf.*, San Antonio, TX, USA, Jun. 2007, pp. 1–5.

[8] R. A. Hanna, W. Hiscock, and P. Klinowski, "Failure analysis of three slow-speed induction motors for reciprocating load application," *IEEE Trans. Ind. Appl.*, vol. 43, no. 2, pp. 429–435, Mar./Apr. 2007.

[9] G. Stojicic, M. Samonig, P. Nussbaumer, G. Joksimovic, M. Vasak, N. Peric, and T. Wolbank, "A method to detect missing magnetic slot wedges in ac machines without disassembling," in *Proc. 37th Annu. IEEE IECON*, Nov. 7–10, 2011, pp. 1698–1703.

Goran Stojčić received the B.Sc. degree in electrical engineering and the M.Sc. degree in power engineering from the Vienna University of Technology, Vienna, Austria, in 2009 and 2011, respectively, where he is currently working toward the Ph.D. degree.

He is currently a Project Assistant with the Department of Energy Systems and Electrical Drives, Vienna University of Technology. His special fields of interest are fault detection and condition monitoring of inverter-fed drives.

Mario Vašak (M'07) received the Ph.D. degree in electrical engineering from the University of Zagreb Faculty of Electrical Engineering and Computing (UNIZG-FER), Zagreb, Croatia, in 2007.

He is currently an Assistant Professor with the Department of Control and Computer Engineering, UNIZG-FER. He works in the areas of predictive/robust/fault-tolerant control and computational geometry applied to the following application domains: renewable energy systems, water management systems, energy-efficient buildings, energy-efficient railway transportation, and automotive systems. On behalf of UNIZG-FER, he led the FP7-SEE-ERA.net PLUS research project MONGS on generator-fault-tolerant control in wind turbines, and currently, he is the UNIZG-FER leader of the FP7-STREP UrbanWater that deals with fresh water supply system management in urban environments. He has published over 50 papers in journals and conference proceedings.

Nedjeljko Perić (M'94–SM'04) received the B.Sc., M.Sc., and Ph.D. degrees in electrical engineering from the University of Zagreb Faculty of Electrical Engineering and Computing (UNIZG-FER), Zagreb, Croatia, in 1973, 1980, and 1989, respectively.

From 1973 to 1993, he was with the Institute of Electrical Engineering, Končar Corporation, Zagreb, as an R&D Engineer, the Head of the Positioning Systems Department, and the Manager of the Automation Section. In 1993, he joined the Department of Control and Computer Engineering at UNIZG-FER as an Associate Professor. He was appointed as a Full Professor in 1997, and since 2010, he has served as the UNIZG-FER Dean. His current research interests are in the fields of process identification and advanced control techniques.

Prof. Perić is a Fellow of the Croatian Academy of Engineering and a member of several international professional associations.

Gojko Joksimović (M'98–SM'11) received the Ph.D. and Full Professor degrees from the University of Montenegro, Podgorica, Montenegro, in 2000 and 2011, respectively.

He is currently with the Faculty of Electrical Engineering, University of Montenegro. His main research areas include the analysis of electrical machines, condition monitoring of electrical machines, and power electronics and control. He is the author of a few books and more than 50 papers published in leading international scientific journals and international conference proceedings.

Thomas M. Wolbank (M'99) received the doctoral degree and the habilitation (Associate Professor degree) from the Vienna University of Technology, Vienna, Austria, in 1996 and 2004, respectively.

He is currently with the Department of Energy Systems and Electrical Drives, Vienna University of Technology. He has coauthored more than 100 papers published in refereed journals and international conference proceedings. His research interests include saliency-based sensorless control of ac drives, dynamic properties and condition monitoring of inverter-fed machines, transient electrical behavior of ac machines, and motor drives and their components and controlling them by the use of intelligent control algorithms.